Cell Metabolism, Volume *31*

Supplemental Information

Pharmacological Activation of Pyruvate Kinase M2 Inhibits $CD4^+$ T Cell Pathogenicity and Suppresses Autoimmunity

Stefano Angiari, Marah C. Runtsch, Caroline E. Sutton, Eva M. Palsson-McDermott, Beth Kelly, Nisha Rana, Harry Kane, Gina Papadopoulou, Erika L. Pearce, Kingston H.G. Mills, and Luke A.J. O'Neill

SUPPLEMENTARY FIGURE TITLES AND LEGENDS

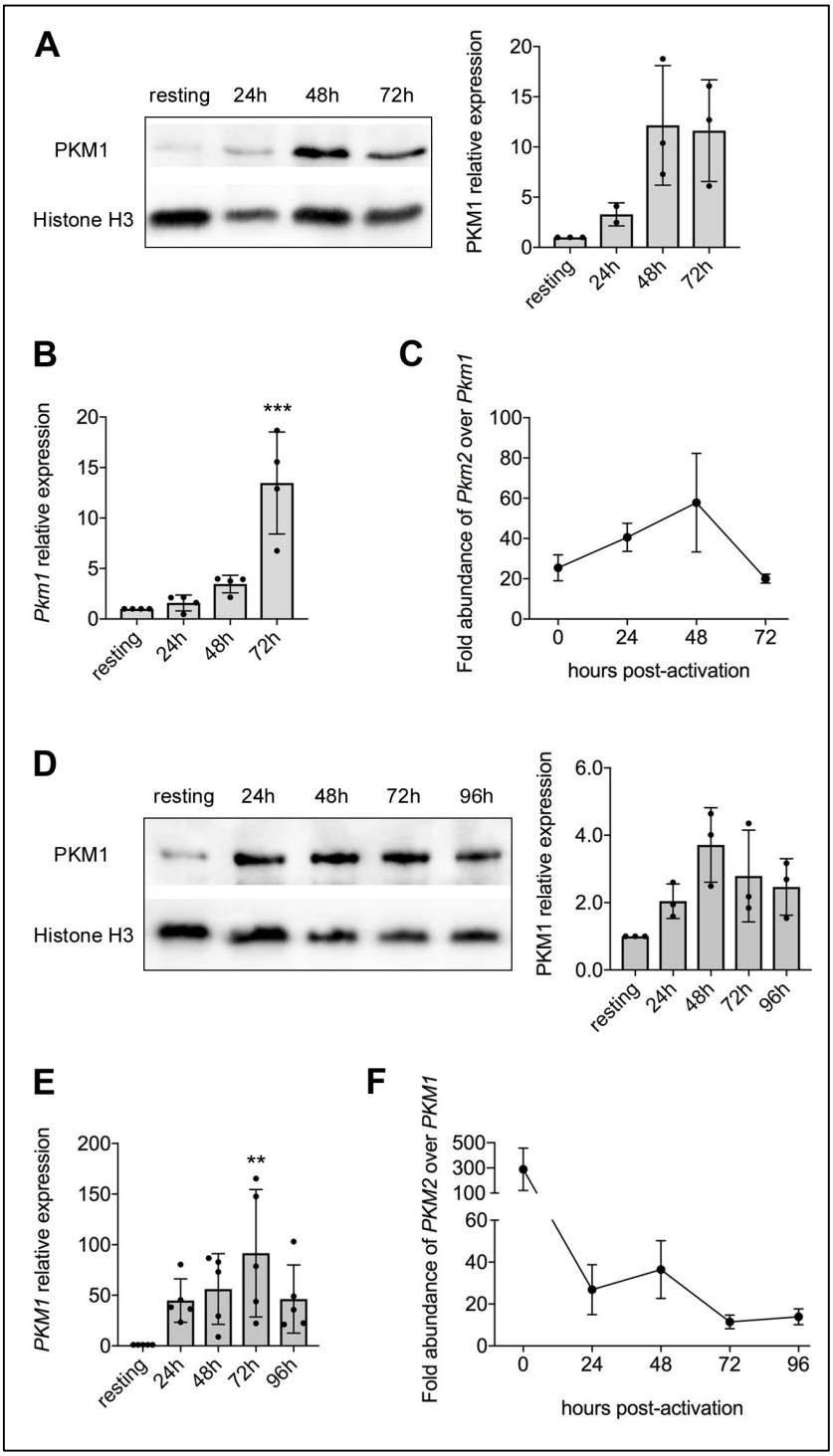

Figure S1. PKM1 expression in resting and activated murine and human CD4$^+$ T cells. Related to Figure 1 and 7. (**A-C**) Murine CD4$^+$CD62$^+$ T cells were stimulated *in vitro* for 3 days with CD3/CD28 antibodies and collected at different time points of activation. (**A**) Left: western blot showing upregulation of PKM1 protein in murine CD4$^+$ T cells following activation. Right: quantification of PKM1 expression by densitometry analysis (n=3 from two independent

experiments). (**B**) Quantification of *Pkm1* mRNA expression in resting versus activated murine $CD4^+$ T cells by qRT-PCR (n=4 from three independent experiments). ***P<0.001 compared to resting condition, by one-way Anova with Dunnett's post-hoc test. (**C**) Fold abundance of *Pkm2* over *Pkm1* mRNA in resting and activated murine $CD4^+$ T cells (n=4-6 from three-four independent experiments). (**D-F**) Human naïve $CD4^+$ T cells were stimulated *in vitro* for 4 days with anti-CD3/CD28 antibodies and collected at different time points of activation. (**E**) Left: western blot showing upregulation of PKM1 protein in human $CD4^+$ T cells following activation. Right: quantification of PKM1 expression by densitometry analysis (n=3 from three independent experiments). (**F**) Quantification of *Pkm1* mRNA expression in human $CD4^+$ T cells by qRT-PCR (n=5 from three independent experiments). **P<0.01 compared to resting condition, by one-way Anova with Dunnett's post-hoc test. (**C**) Fold abundance of *PKM2* versus *PKM1* expression levels in resting and activated human $CD4^+$ T cells (n=5 from three independent experiments). For all panels, data are the mean ± SD.

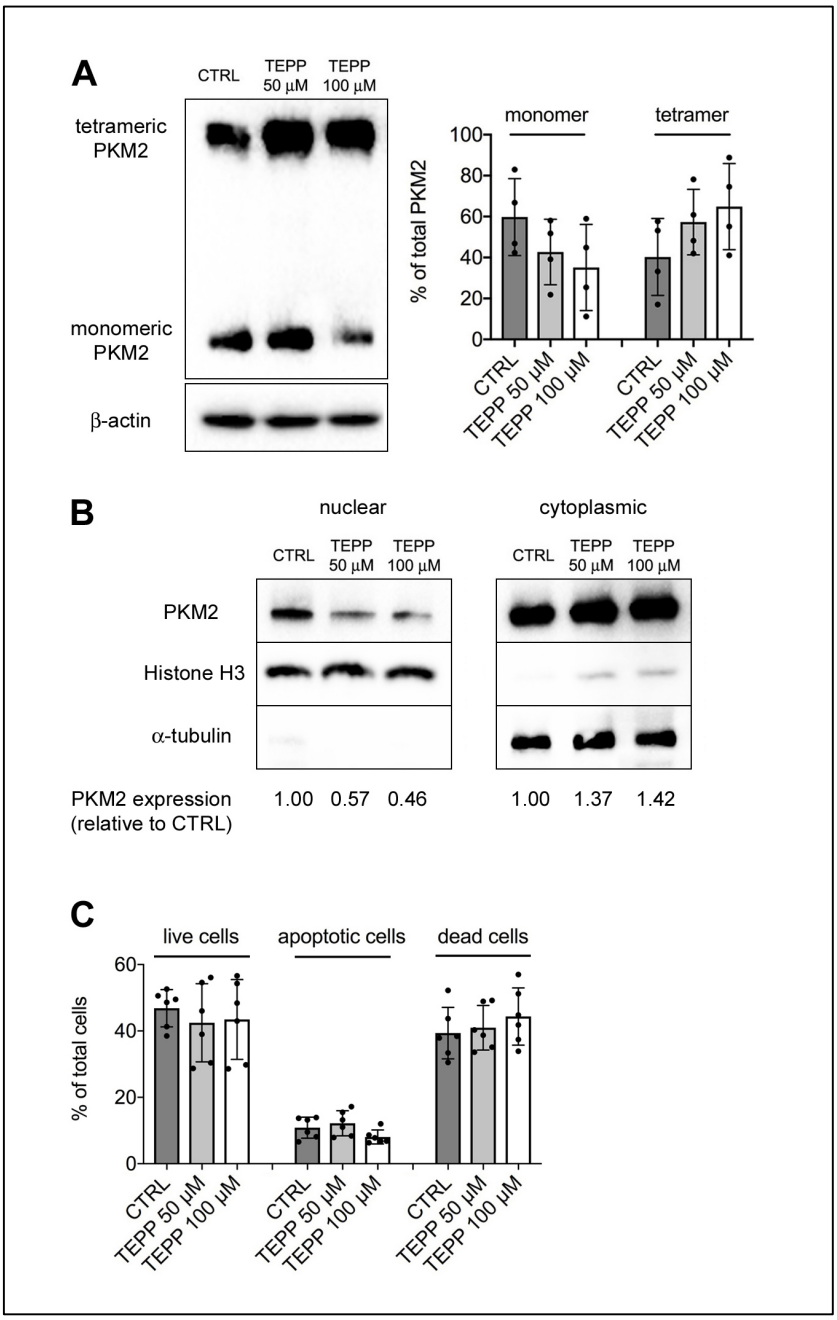

Figure S2. Effect of TEPP-46 on PKM2 tetramerisation, PKM2 nuclear translocation and T cell viability. Related to Figure 2. (**A**) Cells were collected after 3 days of stimulation, crosslinked with DSS and analysed for PKM2 expression. Left: Representative western blot showing induction of PKM2 tetrameric isoform by TEPP-46. Right: quantification of relative tetrameric and monomeric isoform expression over total PKM2 by densitometry analysis (n=4 from three independent experiments). (**B**) Cells were collected after 2 days of stimulation and PKM2 expression in nucleus and cytoplasm was analysed by western blot after cell fractionation. One representative experiment out of three showing a dose-dependent reduction of nuclear PKM2 expression in cells treated with TEPP-46 is displayed. (**C**) Murine $CD4^+$ T cells were collected after

3 days of activation in the presence of TEPP-46. Cells were stained with PI and Annexin V (AV) to determine live (PI^-AV^-), apoptotic (PI^-AV^+) or necrotic/dead cells (PI^+AV^+) (n=6 from three independent experiments). For all panels, data are the mean ± SD.

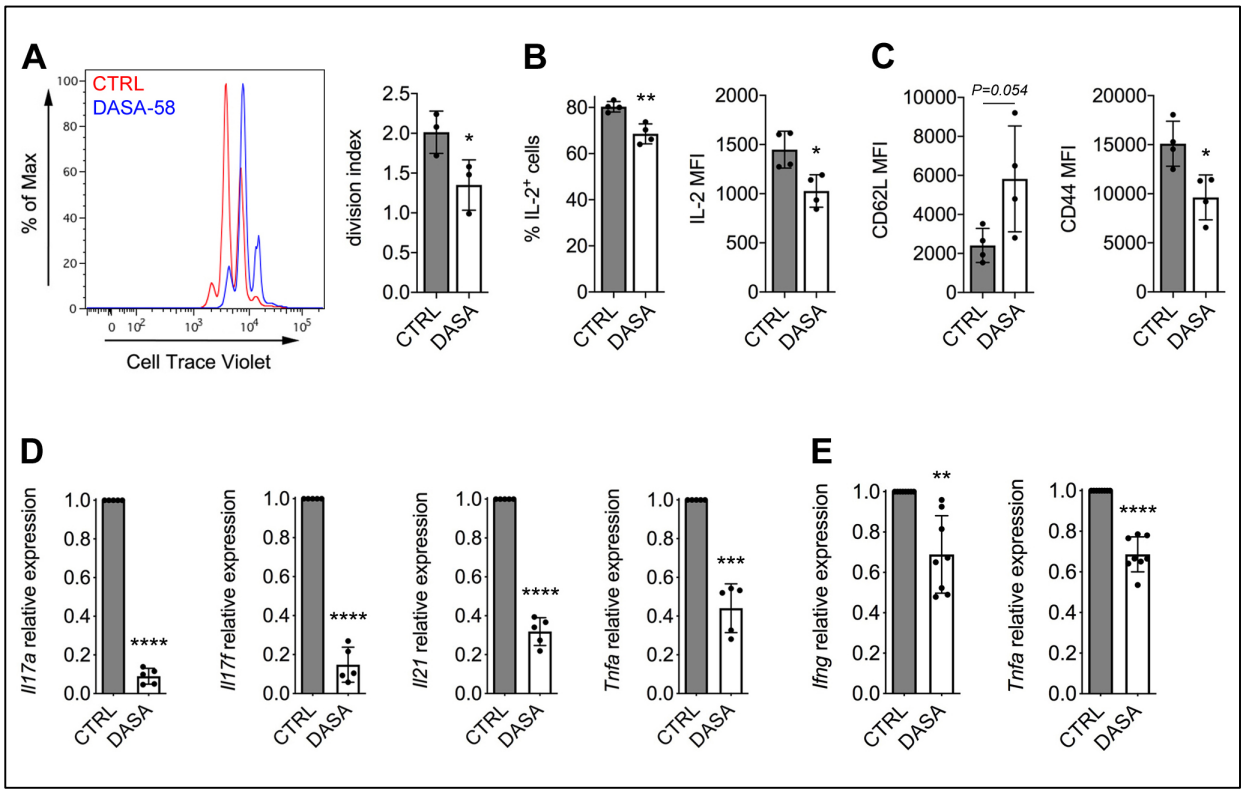

Figure S3. Effect of DASA-58 on CD4$^+$ T cell activation and generation of Th17 and Th1 cells *in vitro*. Related to Figure 2, Figure 4 and Figure 5. (**A-C**) Murine CD4$^+$CD62$^+$ T cells were activated *in vitro* with CD3/CD28 antibodies in the presence of DMSO (CTRL condition) or DASA-58 25 µM. (**A**) Cells were collected after 3 days of stimulation. Left: representative flow cytometry plot displaying T cell proliferation assessed as CellTrace^{TM} Violet dilution. Right: quantification of division index by FlowJo software (n=3 from two independent experiments). (**B**) Percentage of IL-2-producing cells and IL-2 MFI in CTRL versus DASA-58-treated cells 24 hours upon activation (n=4 from two independent experiments). (**C**) MFI of surface CD62L and CD44 expression, evaluated by flow cytometry. (n=4 from two independent experiments). (**D**) Murine CD4$^+$CD62$^+$ T cells were activated *in vitro* under Th17-polarising conditions in the presence of DMSO (CTRL condition) or DASA-58 100 µM. Expression of *Il17a*, *Il17f*, *Il21* and *Tnfa* mRNA in CTRL and DASA-treated Th17 cells was quantified by qRT-PCR (n=5 from two independent experiments). (**E**) Murine CD4$^+$CD62$^+$ T cells were activated *in vitro* under Th1-polarising conditions in the presence of DMSO (CTRL condition) or DASA-58 25 µM. Expression of *Ifng* and *Tnfa* mRNA in CTRL and DASA-treated Th1 cells was quantified by qRT-PCR (n=8 from three independent experiments). For all panels, data are the mean ± SD. *P<0.05, ** P<0.01, ***P<0.001 or ****P<0.0001 compared to CTRL condition, by unpaired (**A-C**) or paired (**D-E**) Student's t test.

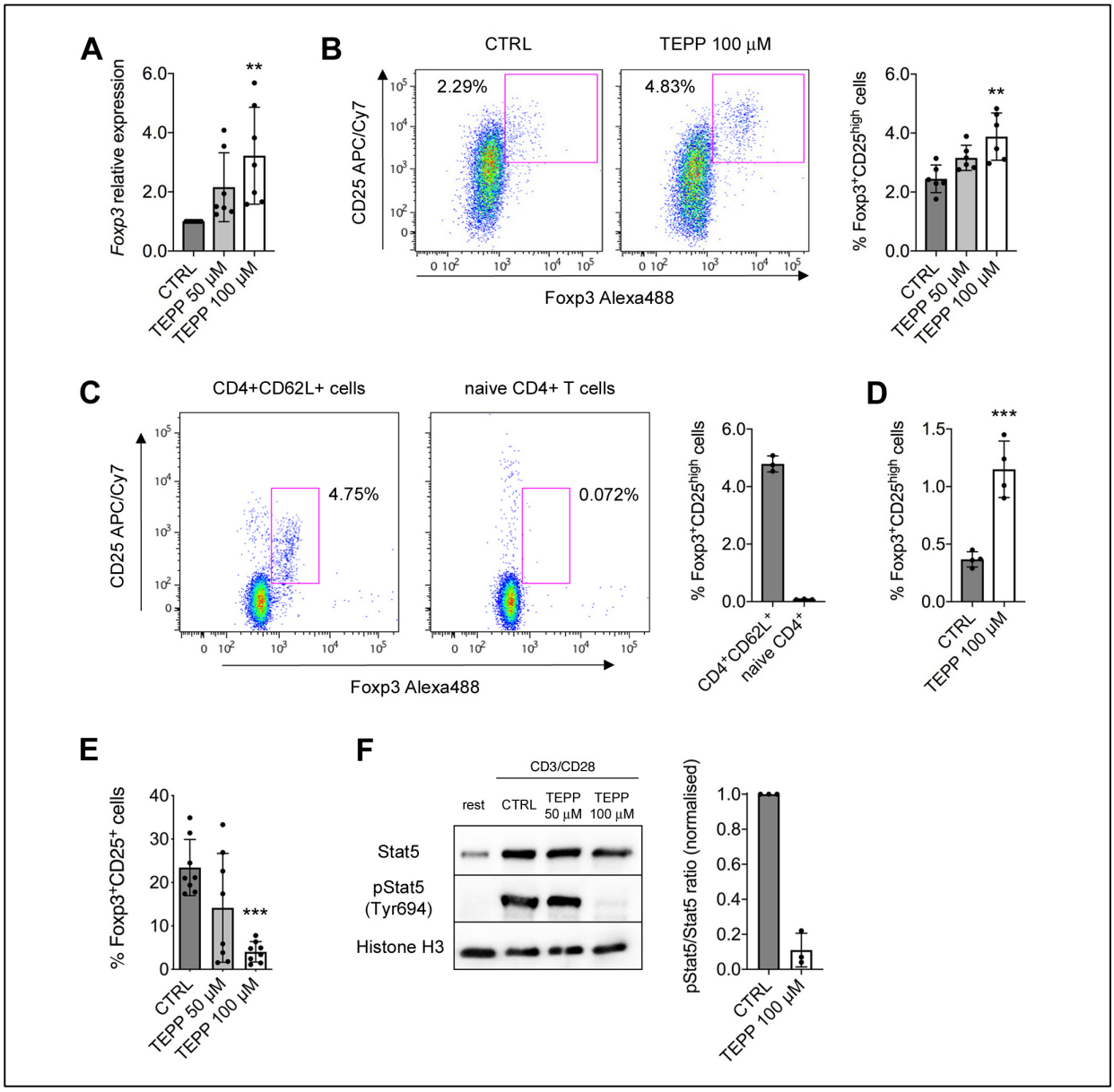

Figure S4. Induction of Foxp3$^+$CD25$^+$ T cells by TEPP-46 and effect of TEPP-46 on TGF-β-induced Tregs. Related to Figure 2. (**A**) Quantification of *Foxp3* mRNA levels by qRT-PCR in murine CD4$^+$ T cells activated in the presence of DMSO (CTRL condition) or TEPP-46 (n=7 from six independent experiments). (**B**) Left: representative plot showing induction of Foxp3$^+$CD25$^+$ T cells by TEPP-46 treatment. Right: quantification of the percentage of Foxp3$^+$CD25$^+$ T cells in CTRL and TEPP-46-treated cells (n=6 from four independent experiments). (**C**) Left: representative flow cytometry plots showing Foxp3$^+$CD25$^+$ T cells in freshly-isolated CD4$^+$CD62L$^+$ resting T cells and naïve CD4$^+$ T cells. Right: quantification of Foxp3$^+$CD25$^+$ T cell percentage in the two populations (n=3). (**D**) Naïve CD4$^+$ T cells were activated with CD3/CD28 antibodies in the presence of TEPP-46. The percentage of Foxp3$^+$CD25$^+$ T cells was evaluated after 3 days of stimulation. (n=4 from 2 independent experiments). (**E**) Murine CD4$^+$CD62$^+$ T cells were activated

in vitro with CD3/CD28 antibodies under Treg-polarising conditions, in the presence of TEPP-46. The percentage of $Foxp3^{+}CD25^{+}$ T cells in CTRL and TEPP-46-treated cells was quantified by flow cytometry (n=8 from four independent experiments). **(F)** Analysis of Stat5 phosphorylation in TGF-β-induced Tregs. Left: western blot showing block of Stat5 phosphorylation by TEPP-46. Right: quantification of phospho-Stat5/Stat5 ratio by densitometry analysis (n=3 from three independent experiments). In all panels, data are the mean the mean ± SD. $^{**}P<0.01$ or $^{***}P<0.001$, compared to CTRL condition, by one-way Anova with Dunnett's post-hoc test (**A, B** and **E**) or unpaired Student's t test (**D**).

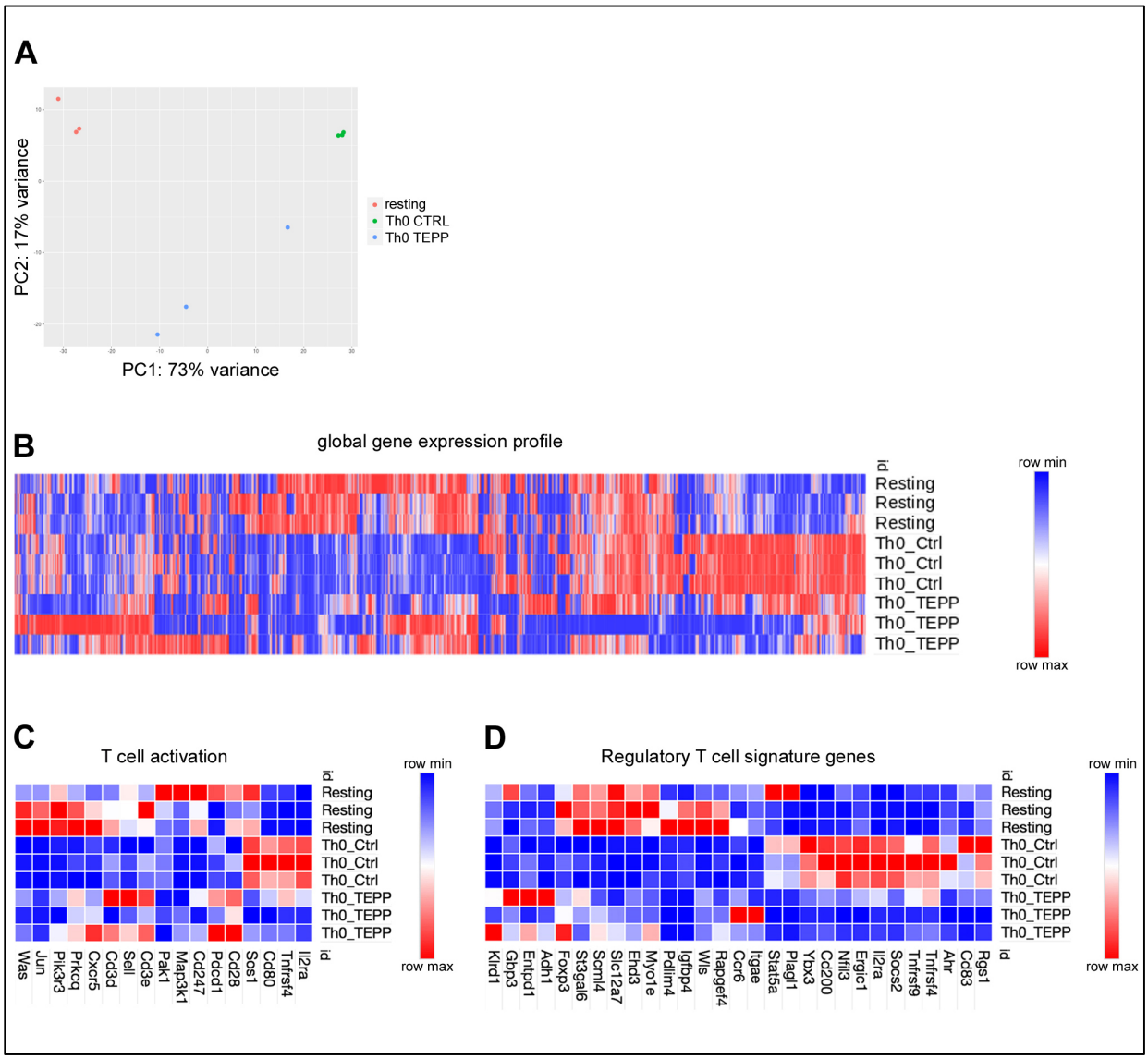

Figure S5. Global expression profile of resting CD4$^+$ T cells and CD4$^+$ T cells activated in the presence of DMSO (Th0 Ctrl) or TEPP-46 100 µM (Th0 TEPP). Related to Figure 2 and Figure 3. (**A**) Plot showing Principal Component analysis of global gene expression in the three T cell populations. (**B**) Heat map showing an overview of global gene expression in resting and Th0 Ctrl or Th0 TEPP-46 cells. (C) Heat map showing expression of genes related to T cells activation in the three populations. (D) Heat map showing expression of regulatory T cell signature genes in the three populations.

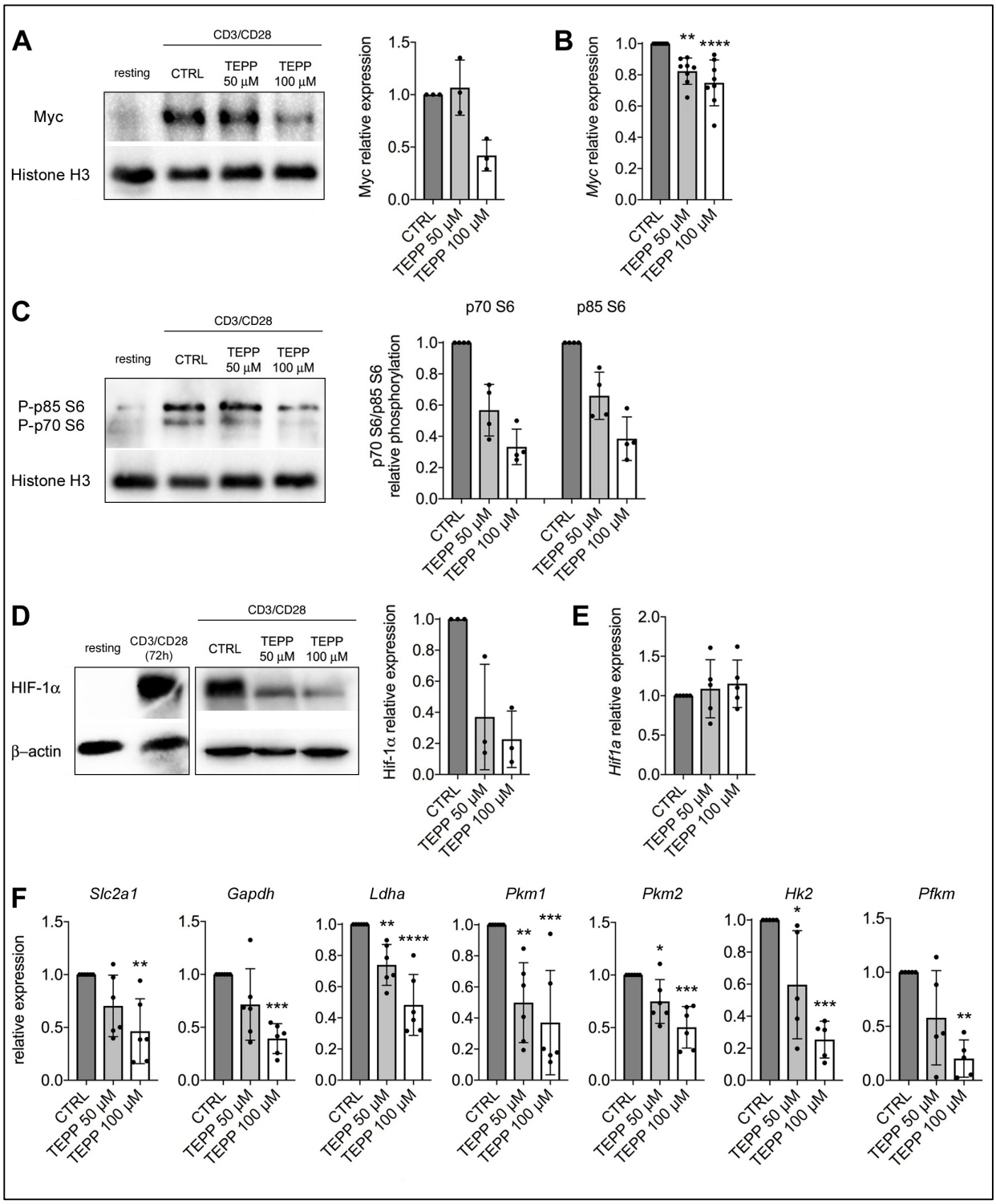

Figure S6. Effect of TEPP-46 on Myc and Hif-1α expression, mTORC1 activity and expression of glycolytic genes in activated T cells. Related to Figure 3. (**A** and **B**) Murine $CD4^+$ T cells were collected after 24 hours of *in vitro* activation with CD3/CD28 antibodies in the presence of DMSO (CTRL condition) or TEPP-46. (**A**) Left: western blot image showing reduction of Myc expression by TEPP-46 treatment. Right: quantification of relative Myc expression in

CTRL and TEPP-46-treated cells by densitometry analysis (n=3 from two independent experiments). (**B**) Quantification of *Myc* mRNA levels in CTRL and TEPP-46-treated cells by qRT-PCR (n=8 from 5 independent experiments). (**C**) Left: image from one representative experiment showing reduction of p70 S6 and p85 S6 phosphorylation by TEPP-46. Right: quantification of relative P-p70 S6 and P-p85 S6 band intensity by densitometry analysis (n=4 from two independent experiments). (**D-F**) Murine $CD4^+$ T cells were collected after 3 days of *in vitro* activation in the presence of DMSO or TEPP-46. (**D**) Left: western blot image showing Hif-1α downregulation in TEPP-46-treated cells, compared to CTRL cells. Right: quantification of relative Hif-1α expression by densitometry analysis (n=3 from two independent experiments). (**E**) *Hif1a* mRNA expression in CTRL and TEPP-46-treated cells quantified by qRT-PCR (n=5 from five independent experiments). (**F**) Expression of glycolytic genes in CTRL and TEPP-46-treated T cells by qRT-PCR (n=5-6 from 5 independent experiments). For all panels, data are the mean ± SD. **P*<0.05, ***P*<0.01, ****P*<0.001 or *****P*<0.0001, compared to CTRL condition, by one-way Anova with Dunnett's post-hoc test.

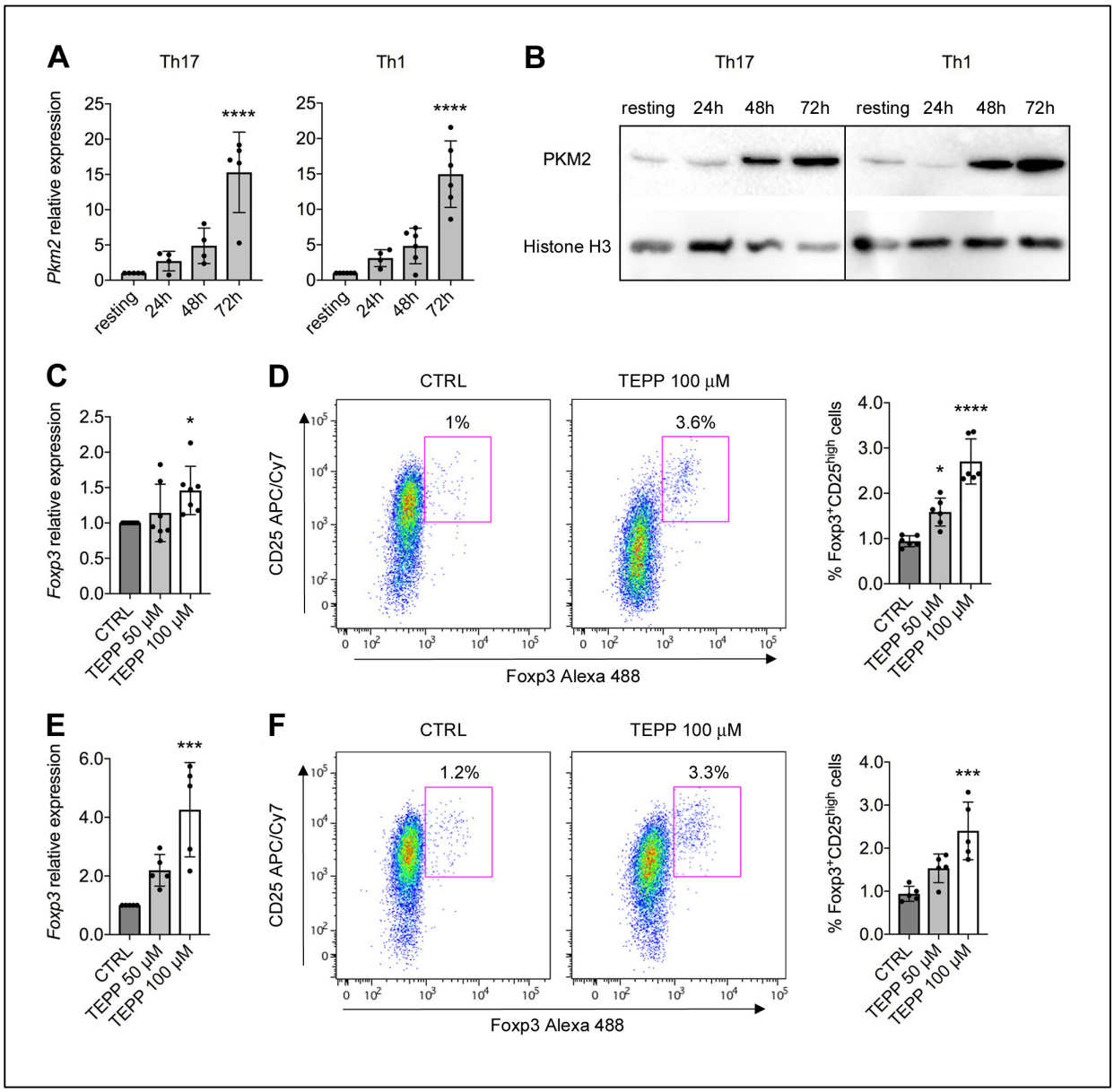

Figure S7. Expression of PKM2 in murine Th17 and Th17 cells and induction of Tregs under Th17 and Th17 polarising-conditions *in vitro*. Related to Figure 4 and 5. Murine $CD4^+CD62^+$ T cells were activated *in vitro* for 3 days with CD3/CD28 antibodies under Th17- or Th1-polarising conditions. (**A**) Quantification of *Pkm2* mRNA expression levels in resting $CD4^+CD62L^+$ T cells versus Th17 and Th1 cells at different time points of activation by qRT-PCR (n=4-6 from four independent experiments). (**B**) Western blot showing upregulation of PKM2 protein in Th17 and Th1 cells following activation. A representative experiment out of two is shown. (**C**) *Foxp3* gene expression in CTRL versus TEPP-46-treated Th17 cells (n=7 from four independent experiments). (**D**) Left: representative plot showing induction of $Foxp3^+CD25^+$ T cells under Th17-polarising conditions by TEPP-46. Right: quantification of the percentage of $Foxp3^+CD25^+$ T cells in CTRL and TEPP-46-treated cell populations (n=6 from two independent experiments). (**E**) *Foxp3*

expression in CTRL versus TEPP-46-treated Th1 cells (n=5 from three independent experiments). (**F**) Left: representative plot showing induction of $Foxp3^{+}CD25^{+}$ T cells by TEPP-46 under Th1-polarising conditions. Right: quantification of the percentage of $Foxp3^{+}CD25^{+}$ T cells in CTRL and TEPP-46-treated cell populations (n=5 from two independent experiments). For all panels, data are the mean ± SD. **P*<0.05, ****P*<0.001 or *****P*<0.0001, compared to CTRL condition, by one-way Anova with Dunnett's post-hoc test.